Chapter 5

Inverse Kinematics for Position

The problem of inverse kinematics is to find the joint angles, given the end effector position and orientation. In general, inverse kinematics is much harder than forward kinematics. Sometimes no analytical solution is possible, and an iterative search is required. Even with analytical solutions possible, multiple solutions arise from which one must pick. In the case of redundant manipulators, there are infinitely many solutions from which to choose. Another complication is that workspace limits may be violated (the point is outside the reach of the manipulator, or joint limits are exceeded).

5.1 Two-link Planar Manipulator

The simplest non-trivial manipulator for which to study inverse kinematics is the planar two-link manipulator (Figure 5.1). Moreover, parts of some spatial manipulators have this structure as a subchain, and the following solution applies to the analysis of those manipulators' inverse kinematics as we shall see later.

First solve for θ_2 using Figure 5.1(A). From the cosine rule,

$$\begin{aligned} x^2 + y^2 &= a_1^2 + a_2^2 - 2a_1 a_2 \cos(\pi - \theta_2) \\ \cos\theta_2 &= \frac{x^2 + y^2 - a_1^2 - a_2^2}{2a_1 a_2} \end{aligned} \tag{5.1}$$

As usual, we should try to avoid using the arccos function because of inaccuracy. Instead, the following half-angle formula is employed:

$$\tan^2\frac{\theta_2}{2} = \frac{1-\cos\theta_2}{1+\cos\theta_2} = \frac{2a_1a_2 - x^2 - y^2 + a_1^2 + a_2^2}{2a_1a_2 + x^2 + y^2 - a_1^2 - a_2^2} = \frac{(a_1+a_2)^2 - (x^2+y^2)}{(x^2+y^2) - (a_1-a_2)^2} \tag{5.2}$$

The second joint angle θ_2 is then found accurately as:

$$\theta_2 = \pm 2\tan^{-1}\sqrt{\frac{(a_1+a_2)^2 - (x^2+y^2)}{(x^2+y^2) - (a_1-a_2)^2}} \tag{5.3}$$

Because of the square root, two solutions result: elbow up and elbow down (Figure 5.1). We pick one of the two solutions to proceed.

Next we will find θ_1, which is determined uniquely given θ_2. From Figure 5.1 we get the relation:

$$\theta_1 = \phi - \psi \tag{5.4}$$

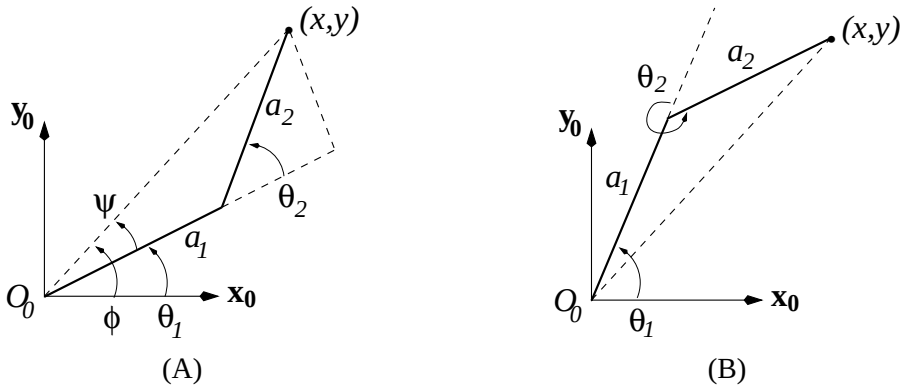

Figure 5.1: Inverse kinematics for two-link planar manipulator. Elbow down (A) and elbow up (B) solutions.

where ϕ is the angle between the radial line to the endpoint and the x axis, and ψ is the angle between link 1 and the radial line. These two angles are found uniquely from

$$\phi = \text{atan2}(y, x) \tag{5.5}$$

$$\psi = \text{atan2}(a_2 \sin\theta_2, a_1 + a_2 \cos\theta_2) \tag{5.6}$$

Note the two different solutions for θ_1 corresponding to the elbow-down versus elbow-up configurations (Figure 5.1).

5.1.1 Alternate Solution

Two arctangent functions are involved to find θ_1 in (5.4). There is an alternate solution based on Gaussian elimination that requires only one arctangent evaluation, which may be more efficient on a computer. The forward kinematics can be written by inspection or by referring to Chapter 2:

$$x = a_1 \mathrm{c}\theta_1 + a_2 \mathrm{c}(\theta_1 + \theta_2) \tag{5.7}$$

$$y = a_1 \mathrm{s}\theta_1 + a_2 \mathrm{s}(\theta_1 + \theta_2) \tag{5.8}$$

Take two different linear combinations of these equations to produce after simplification:

$$x\mathrm{c}\theta_1 + y\mathrm{s}\theta_1 = a_1 + a_2 \mathrm{c}\theta_2 \tag{5.9}$$

$$x\mathrm{s}\theta_1 - y\mathrm{c}\theta_1 = -a_2 \mathrm{s}\theta_2 \tag{5.10}$$

There are now two equations to solve for $\mathrm{s}\theta_1$ and $\mathrm{c}\theta_1$ separately using Gaussian elimination.

$$\mathrm{c}\theta_1 = \frac{x(a_1 + a_2\mathrm{c}\theta_2) + y(a_2\mathrm{s}\theta_2)}{x^2 + y^2} \tag{5.11}$$

$$\mathrm{s}\theta_1 = \frac{y(a_1 + a_2\mathrm{c}\theta_2) - x(a_2\mathrm{s}\theta_2)}{x^2 + y^2} \tag{5.12}$$

The 4-quadrant arctangent is then applied only once to find θ_1.

5.2 Spatial 3-DOF Manipulators

Manipulators can often be considered to be composed of two parts. The first 3 joints form a regional structure whose primary purpose is to position the wrist in space. The last 3 joints form the orienting structure whose purpose is to orient the hand or grasped object. In this section, we will solve the inverse kinematics of the first three degrees of freedom of the elbow robot of the previous chapter, assuming that the wrist position is given. A planar two-link manipulator often makes up the last two links of the regional structure, and it will be seen that the solution of the previous section can be directly applied.

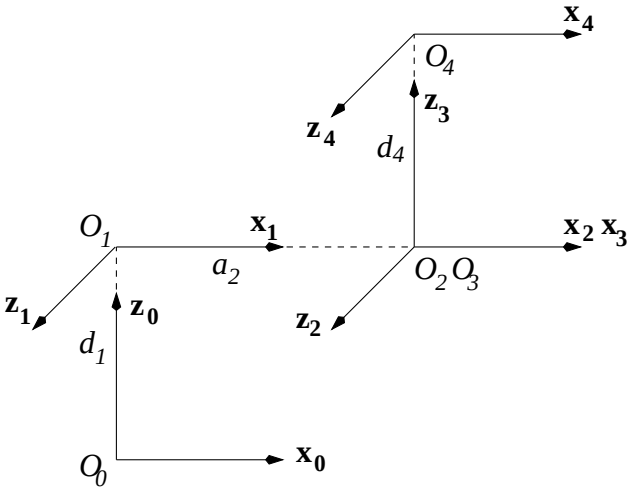

i	a_i	d_i	α_i
1	0	d_1	$\pi/2$
2	a_2	0	0
3	0	0	$-\pi/2$
4	0	d_4	$\pi/2$

Figure 5.2: First four joints of the elbow robot.

5.2.1 The Elbow Robot Regional Structure

The DH parameters for the first 4 links are shown in Figure 5.2. The link 4 parameters have been included in the regional structure because they locate the wrist point O_4, which we assume is known relative to O_0, i.e., ${}^0\mathbf{d}_{04} = O_4 - O_0$. Although $\mathbf{z}_3$ and $\mathbf{z}_4$ are rotation axes, they have no influence on the wrist position O_4 because they pass through that point. For the purposes of this section, they can be considered inactive.

Project the position of the wrist point into the x_0, y_0 plane, i.e., just select the x, y coordinates of ${}^0\mathbf{d}_{04}$ (Figure 5.3(A)). The radial line from O_0 to this projected point is parallel to $\mathbf{x}_1$. Hence the angle between this radial line and $\mathbf{x}_0$ is θ_1:

$$\theta_1 = \tan^{-1}\left(\frac{{}^0d_{04y}}{{}^0d_{04x}}\right) \tag{5.13}$$

Because of the arctangent function, there are two possible solutions for θ_1. These correspond to "lefty" and "righty" configurations: starting from one of these configurations, the base rotates 180 degrees while the upper arm rotates over the top to achieve the same wrist position. In Figure 5.3(A), this corresponds to the $\mathbf{x}_1$ axis pointing in the other direction; the two θ_1 solutions differ by π. For manipulators such as the PUMA which have an offset in the shoulder, the result is the left versus right arm look; this case is treated below.

Next, find the vector ${}^1\mathbf{d}_{14}$ from coordinate origin 1 to the wrist. We can express the result with respect to the orientation of frame 1 because we now know θ_1.

$${}^1\mathbf{d}_{14} = {}^1\mathbf{d}_{04} - {}^1\mathbf{d}_{01} = {}^0\mathbf{R}_1^T({}^0\mathbf{d}_{04} - {}^0\mathbf{d}_{01}) \tag{5.14}$$

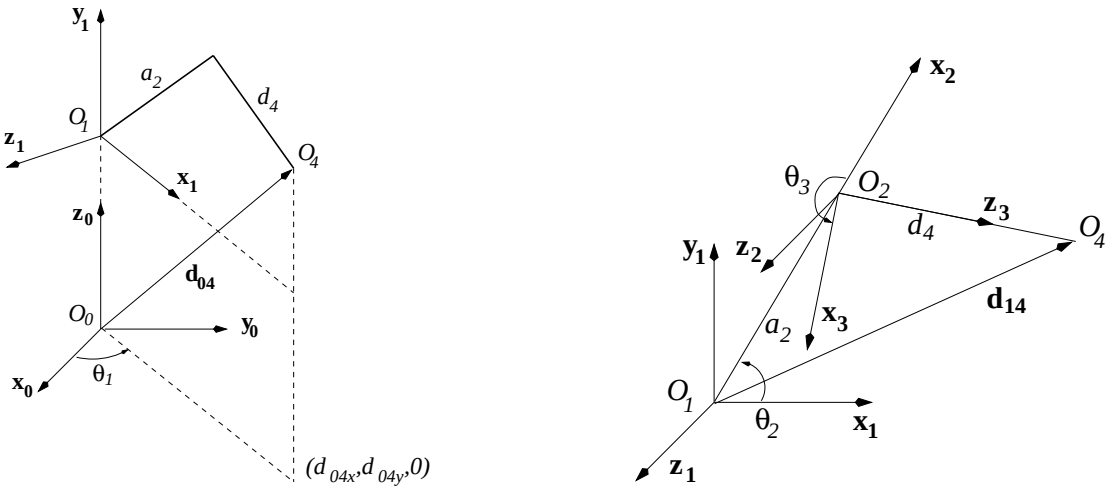

Figure 5.3: (A) Solution for θ_1. (B) Solution for θ_2 and θ_3.

where

$$ {}^0\mathbf{R}_1 = \begin{bmatrix} \mathrm{c}\theta_1 & -\mathrm{s}\theta_1\mathrm{c}\alpha_1 & \mathrm{s}\theta_1\mathrm{s}\alpha_1 \\ \mathrm{s}\theta_1 & \mathrm{c}\theta_1\mathrm{c}\alpha_1 & -\mathrm{c}\theta_1\mathrm{s}\alpha_1 \\ 0 & \mathrm{s}\alpha_1 & \mathrm{c}\alpha_1 \end{bmatrix} = \begin{bmatrix} \mathrm{c}\theta_1 & 0 & \mathrm{s}\theta_1 \\ \mathrm{s}\theta_1 & 0 & -\mathrm{c}\theta_1 \\ 0 & 1 & 0 \end{bmatrix} \tag{5.15} $$

since $\alpha_1 = \pi/2$. Hence

$$ {}^1\mathbf{d}_{14} = \begin{bmatrix} \mathrm{c}\theta_1 & \mathrm{s}\theta_1 & 0 \\ 0 & 0 & 1 \\ \mathrm{s}\theta_1 & -\mathrm{c}\theta_1 & 0 \end{bmatrix} \left(\begin{bmatrix} {}^0d_{04x} \\ {}^0d_{04y} \\ {}^0d_{04z} \end{bmatrix} - d_1 \begin{bmatrix} 0 \\ 0 \\ 1 \end{bmatrix} \right) = \begin{bmatrix} {}^0d_{04x}\mathrm{c}\theta_1 + {}^0d_{04y}\mathrm{s}\theta_1 \\ {}^0d_{04z} - d_1 \\ {}^0d_{04x}\mathrm{s}\theta_1 - {}^0d_{04y}\mathrm{c}\theta_1 \end{bmatrix} \tag{5.16} $$

The upper arm and forearm lie in the $\mathbf{x}_1, \mathbf{y}_1$ plane. Hence we may apply the results for the inverse kinematics of a planar 2-link manipulator. The only difference is that there is an extra angle $\pi/2$ in addition to θ_3 to locate the forearm (Figure 5.3(B)). Define a new joint angle $\theta_3' = \theta_3 + \pi/2$. Then θ_2, θ_3' exactly correspond to θ_1, θ_2 of the previous section, while the first two components of ${}^1\mathbf{d}_{14}$ correspond to x, y. Hence apply either solution from section 5.1 to find θ_2 and θ_3', and then θ_3.

5.2.2 An Elbow Robot with a Shoulder

As mentioned above, some robots appear to have a shoulder, in that the plane of the upper arm and forearm does not intersect the first rotation axis. The robot of Figure 5.4 is derived from the previous robot by adding an offset d_2, which makes it look like a left arm. From a workspace standpoint, the advantage is that the upper arm will not hit the base when it is straight down.

The shoulder offset makes the calculation of θ_1 more complex, because the $\mathbf{x}_1$ axis is no longer in the vertical plane of the upper arm and forearm (Figure 5.5(A)). When $\mathbf{x}_1$ and the wrist point are projected onto the $\mathbf{x}_0, \mathbf{y}_0$ plane, then the angle θ_1 from $\mathbf{x}_0$ to $\mathbf{x}_1$ is no longer the same as the angle from $\mathbf{x}_0$ to the projected wrist point. The projection on the $\mathbf{x}_0, \mathbf{y}_0$ plane is redrawn in Figure 5.5(B) for clarity. Suppose the wrist

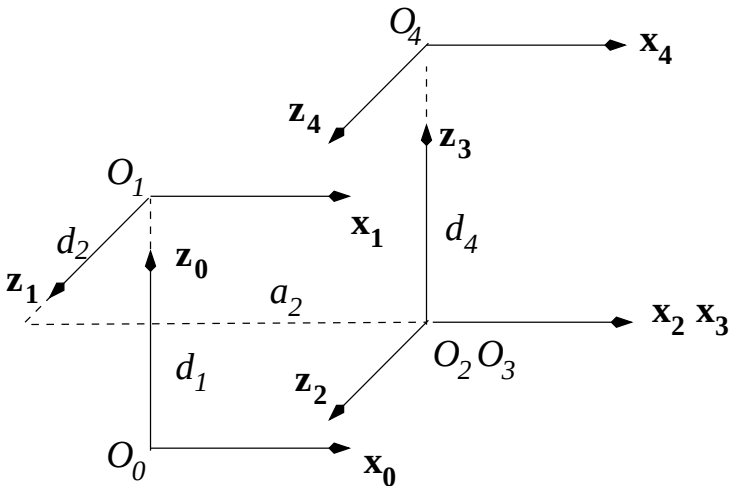

i	a_i	d_i	α_i
1	0	d_1	$\pi/2$
2	a_2	d_2	0
3	0	0	$-\pi/2$
4	0	d_4	$\pi/2$

Figure 5.4: First four joints of the shoulder-elbow robot.

point is (x, y), ϕ is the angle to the radial line of length $r = \sqrt{x^2 + y^2}$ to the wrist point, and ψ is as shown. Then

$$\theta_1 = \phi + (\pi/2 - \psi) \tag{5.17}$$

where

$$\phi = \text{atan2}(y, x) \tag{5.18}$$

$$\cos\psi = d_2/r \tag{5.19}$$

Similar to (5.2), we compute ψ from

$$\tan^2\frac{\psi}{2} = \frac{1-\cos\psi}{1+\cos\psi} = \frac{r-d_2}{r+d_2} \tag{5.20}$$

There are two solutions for ψ and hence for θ_1, which more transparently correspond to "lefty" and "righty."

To find θ_2 and θ_3, we again reduce the problem to that of the planar two-link manipulator by finding the wrist position relative to the shoulder:

$${}^1\mathbf{d}_{14} = {}^0\mathbf{R}_1^T \left({}^0\mathbf{d}_{04} - d_1 \, {}^0\mathbf{z}_0 \right) \tag{5.21}$$

Choose the (x, y) components of ${}^1\mathbf{d}_{14}$ to solve for θ_2, θ_3 as in the previous section. The shoulder offset d_2, which is along the $\mathbf{z}_1$ axis, does not affect these components.

5.3 Spherical Manipulator

The spherical wrist on manipulators primarily serves to orient the last link. When considered by itself, a spherical wrist is called a spherical manipulator or mechanism. Consider again the spherical joint from the previous chapter (Figure 5.6). The numbering of the first joint begins with 4, because as will be seen later the inverse kinematics of the 6 degree-of-freedom elbow robot can be obtained merely by juxtaposing the solutions for the spatial 3R manipulatr and the spherical manipulator.

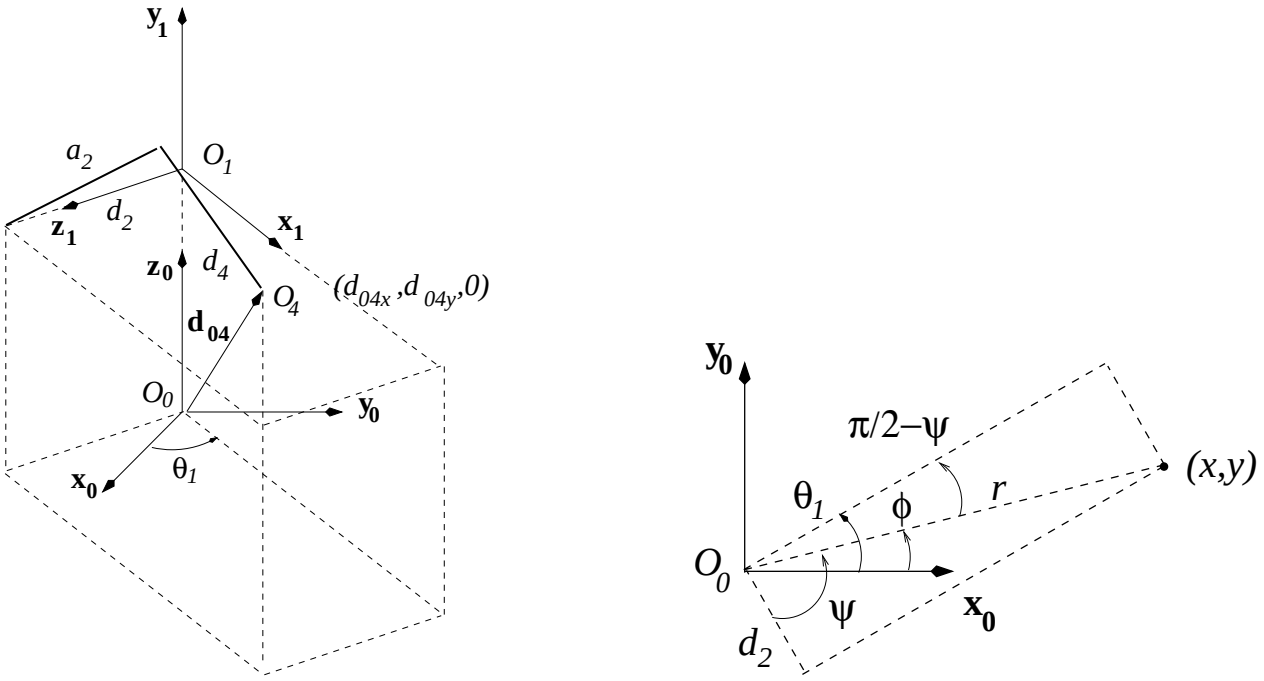

Figure 5.5: (A) A shoulder causes the upper arm/forearm vertical plane not to intersect the origin O_0. (B) Projection of the arm and shoulder onto the $\mathbf{x}_0, \mathbf{y}_0$ plane.

Suppose that the orientation ${}^3\mathbf{R}_6$ of frame 6 relative to frame 3 is given, and we have to find the three joint angles $\theta_4, \theta_5, \theta_6$ to generate ${}^3\mathbf{R}_6$. The offset d_4 of the wrist relative to O_3 does not influence this orientation problem. The solution is more elaborate and less intuitive than the positioning problem for the spatial 3R manipulator, and proceeds through matrix manipulation and simultaneous equations. For simplicity, let r_{ij} represent an element of matrix ${}^3\mathbf{R}_6$. From the definition of ${}^3\mathbf{R}_6$,

$$ {}^3\mathbf{R}_6 = {}^3\mathbf{R}_4 \, {}^4\mathbf{R}_5 \, {}^5\mathbf{R}_6 \tag{5.22} $$

Rather than multiply out the right side, a trick is to solve a simpler problem by solving for θ_4 from

$$ {}^3\mathbf{R}_6 \, {}^5\mathbf{R}_6^T = {}^3\mathbf{R}_4 \, {}^4\mathbf{R}_5 \tag{5.23} $$

This trick separates out θ_6, as can be seen when each side is expanded below.

$$ {}^3\mathbf{R}_4 \, {}^4\mathbf{R}_5 = \begin{bmatrix} \mathrm{c}\theta_4 & 0 & \mathrm{s}\theta_4 \\ \mathrm{s}\theta_4 & 0 & -\mathrm{c}\theta_4 \\ 0 & 1 & 0 \end{bmatrix} \begin{bmatrix} \mathrm{c}\theta_5 & 0 & -\mathrm{s}\theta_5 \\ \mathrm{s}\theta_5 & 0 & \mathrm{c}\theta_5 \\ 0 & -1 & 0 \end{bmatrix} = \begin{bmatrix} \vdots & \vdots & -\mathrm{c}\theta_4\mathrm{s}\theta_5 \\ \vdots & \vdots & -\mathrm{s}\theta_4\mathrm{s}\theta_5 \\ \vdots & \vdots & \mathrm{c}\theta_5 \end{bmatrix} \tag{5.24} $$

where we only care about the last column. Then

$$ {}^3\mathbf{R}_6 \, {}^5\mathbf{R}_6^T = \begin{bmatrix} r_{11} & r_{12} & r_{13} \\ r_{21} & r_{22} & r_{23} \\ r_{31} & r_{32} & r_{33} \end{bmatrix} \begin{bmatrix} \mathrm{c}\theta_6 & \mathrm{s}\theta_6 & 0 \\ -\mathrm{s}\theta_6 & \mathrm{c}\theta_6 & 0 \\ 0 & 0 & 1 \end{bmatrix} = \begin{bmatrix} \vdots & \vdots & r_{13} \\ \vdots & \vdots & r_{23} \\ \vdots & \vdots & r_{33} \end{bmatrix} \tag{5.25} $$

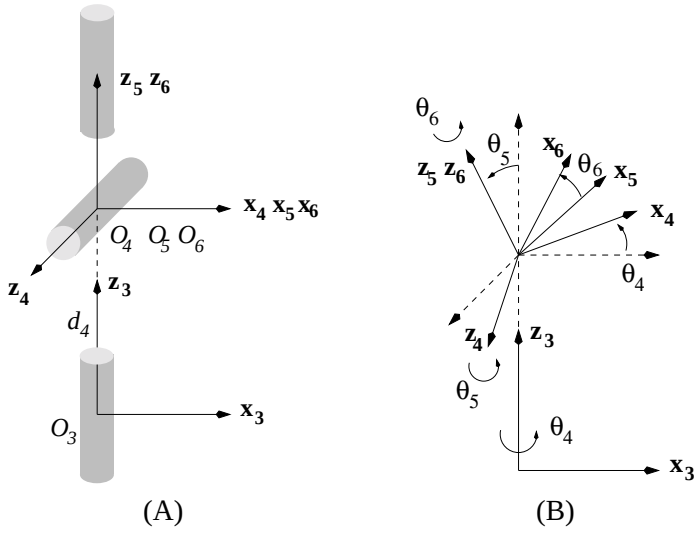

(A) (B)

i	a_i	d_i	α_i	θ_i
4	0	d_4	$\pi/2$	θ_4
5	0	0	$-\pi/2$	θ_5
6	0	0	0	θ_6

Figure 5.6: (A) Spherical joint in zero position. (B) Spherical joint after displacements in all angles.

where again we only care about the last column. Equating corresponding elements,

$$\theta_4 = \tan^{-1}\left(\frac{-r_{23}}{-r_{13}}\right) = \tan^{-1}\left(\frac{\mathrm{s}\theta_4\mathrm{s}\theta_5}{\mathrm{c}\theta_4\mathrm{s}\theta_5}\right) \tag{5.26}$$

There are two possible solutions for θ_4.

However, θ_5 and θ_6 are determined uniquely as evidenced by the use of the 4-quadrant artangent function below. Again from the definition of ${}^3\mathbf{R}_6$,

$$({}^3\mathbf{R}_4)^T\ {}^3\mathbf{R}_6 = {}^4\mathbf{R}_5\ {}^5\mathbf{R}_6 \tag{5.27}$$

where

$$\begin{aligned} {}^4\mathbf{R}_5\ {}^5\mathbf{R}_6 &= \begin{bmatrix} \mathrm{c}\theta_5 & 0 & -\mathrm{s}\theta_5 \\ \mathrm{s}\theta_5 & 0 & \mathrm{c}\theta_5 \\ 0 & -1 & 0 \end{bmatrix} \begin{bmatrix} \mathrm{c}\theta_6 & -\mathrm{s}\theta_6 & 0 \\ \mathrm{s}\theta_6 & \mathrm{c}\theta_6 & 0 \\ 0 & 0 & 1 \end{bmatrix} = \begin{bmatrix} \vdots & \vdots & -\mathrm{s}\theta_5 \\ \vdots & \vdots & \mathrm{c}\theta_5 \\ -\mathrm{s}\theta_6 & -\mathrm{c}\theta_6 & 0 \end{bmatrix} \\ \mathbf{R}_4^T\mathbf{R}_3^6 &= \begin{bmatrix} \mathrm{c}\theta_4 & \mathrm{s}\theta_4 & 0 \\ 0 & 0 & 1 \\ \mathrm{s}\theta_4 & -\mathrm{c}\theta_4 & 0 \end{bmatrix} \begin{bmatrix} r_{11} & r_{12} & r_{13} \\ r_{21} & r_{22} & r_{23} \\ r_{31} & r_{32} & r_{33} \end{bmatrix} \\ &= \begin{bmatrix} \vdots & \vdots & r_{13}\mathrm{c}\theta_4 + r_{23}\mathrm{s}\theta_4 \\ \vdots & \vdots & r_{33} \\ r_{11}\mathrm{s}\theta_4 - r_{21}\mathrm{c}\theta_4 & r_{12}\mathrm{s}\theta_4 - r_{22}\mathrm{c}\theta_4 & r_{13}\mathrm{s}\theta_4 - r_{23}\mathrm{c}\theta_4 \end{bmatrix} \end{aligned} \tag{5.28, 5.29}$$

Hence equating corresponding elements,

$$\begin{aligned} \mathrm{s}\theta_5 &= -r_{13}\mathrm{c}\theta_4 - r_{23}\mathrm{s}\theta_4 \\ \mathrm{c}\theta_5 &= r_{33} \end{aligned} \tag{5.30}$$

$$\begin{aligned} \theta_5 &= \text{atan2}(\text{s}\theta_5, \text{c}\theta_5) \\ \text{s}\theta_6 &= -r_{11}\text{s}\theta_4 + r_{21}\text{c}\theta_4 \\ \text{c}\theta_6 &= -r_{12}\text{s}\theta_4 + r_{22}\text{c}\theta_4 \\ \theta_6 &= \text{atan2}(\text{s}\theta_6, \text{c}\theta_6) \end{aligned} \tag{5.31}$$

When $\theta_5 = 0$ in (5.26), there is a degeneracy called the *wrist singularity.* At this singularity, the $\mathbf{z}_3$ and $\mathbf{z}_5$ rotation axes align (Figure 5.6(A)), resulting in a loss of one degree of freedom. Only the linear combination $\theta_4 + \theta_6$ can be found, a situation analogous to the Euler angle degeneracy.

5.4 Inverse Kinematics of 6-DOF Manipulators

In general, the inverse kinematics of arbitrary 6-DOF rotary manipulators cannot be solved analytically. Under two special cases, however, an analytic solution is possible.

1. There is a spherical joint anywhere in the chain.
2. There is a planar pair anywhere in the chain.

These joints allow the manipulator to be broken into subsystems which are more easily solved.

The elbow manipulator has a spherical wrist, and hence its inverse kinematics may be solved analytically. The DH parameters of the elbow manipulator are repeated in Figure 5.7, where the zero position is also shown. The last frame 6 has been chosen to be coincident with frame 5 when $\theta_6 = 0$.

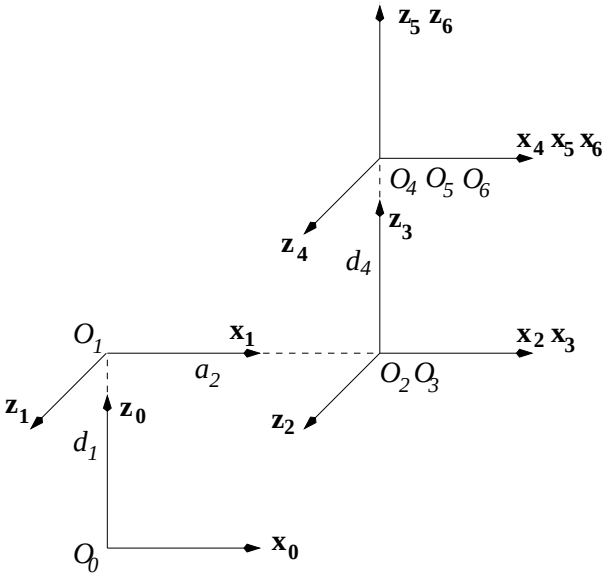

i	a_i	d_i	α_i
1	0	d_1	$\pi/2$
2	a_2	0	0
3	0	0	$-\pi/2$
4	0	d_4	$\pi/2$
5	0	0	$-\pi/2$
6	0	0	0

Figure 5.7: Zero position of elbow robot, and associated DH parameterization.

Suppose the robot is grasping an object, which has a tool frame ${}^6\mathbf{T}_{tool}$ relative to frame 6 (Figure 5.8(A)). Then the endpoint location is:

$${}^0\mathbf{T}_{tool} = \begin{bmatrix} {}^0\mathbf{R}_{tool} & {}^0\mathbf{d}_{tool} \\ \mathbf{0}^T & 1 \end{bmatrix} = {}^0\mathbf{T}_1\ {}^1\mathbf{T}_2 \cdots\ {}^5\mathbf{T}_6\ {}^6\mathbf{T}_{tool} \tag{5.32}$$

The position ${}^0\mathbf{d}_{tool}$ and orientation ${}^0\mathbf{R}_{tool}$ of the tool is somehow given to us, for example from a trajectory planner. Our job is to find the joint angles that realize this tool pose. The solution to the inverse kinematics proceeds by 3 steps.

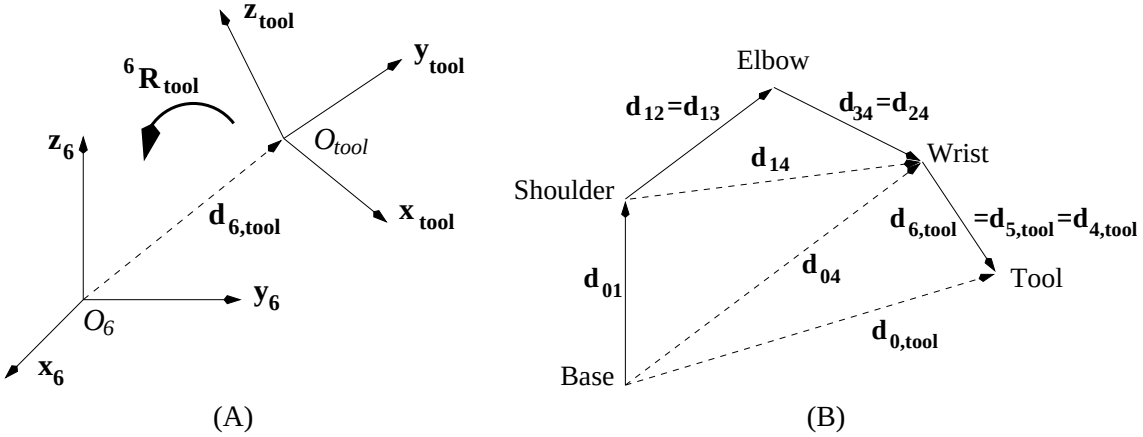

Figure 5.8: (A) Tool frame location relative to frame 6. (B) Inter-frame vectors.

5.4.1 Step 1: Decompose the Manipulator at the Wrist

This is the singly most important step of the procedure. The spherical wrist makes this possible. We find the position of the wrist point, which subsequently is used to solve for the first 3 joint angles. The wrist joint angles are then solved to give the correct orientation. Let the tool transform be given:

$$ {}^6\mathbf{T}_{tool} = \begin{bmatrix} {}^6\mathbf{R}_{tool} & {}^6\mathbf{d}_{6,tool} \\ \mathbf{0}^T & 1 \end{bmatrix} \tag{5.33} $$

Since ${}^6\mathbf{d}_{6,tool}$ is the vector from the wrist to the tool frame origin, it also locates origins O_4 and O_5 which are coincident with O_6. Hence we express the distance from base to wrist as the vector from O_0 to O_4:

$$ {}^0\mathbf{d}_{04} = {}^0\mathbf{d}_{0,tool} - {}^0\mathbf{d}_{6,tool} = {}^0\mathbf{d}_{0,tool} - {}^0\mathbf{R}_{tool}({}^6\mathbf{R}_{tool})^T\,{}^6\mathbf{d}_{6,tool} \tag{5.34} $$

The various inter-frame translation vectors $\mathbf{d}_{ij}$ are shown in Figure 5.8(B).

5.4.2 Step 2: Find the First 3 Joint Angles

We can now simply apply the solution of Section 5.2.1 to find $\theta_1, \theta_2, \theta_3$ given ${}^0\mathbf{d}_{04}$.

5.4.3 Step 3: Find the Last 3 Joint Angles

The first 3 joint angles impart a certain ortientation in space of the forearm. The wrist angles correct for the difference between this orientation and the desired orientation of the end link.

$$ \begin{aligned} {}^0\mathbf{R}_{tool} &= ({}^0\mathbf{R}_1\,{}^1\mathbf{R}_2\,{}^2\mathbf{R}_3)({}^3\mathbf{R}_4\,{}^4\mathbf{R}_5\,{}^5\mathbf{R}_6){}^6\mathbf{R}_{tool} \\ {}^3\mathbf{R}_6 &= ({}^0\mathbf{R}_3)^T\,{}^0\mathbf{R}_{tool}\,{}^6\mathbf{R}_{tool}^T \end{aligned} \tag{5.35} $$

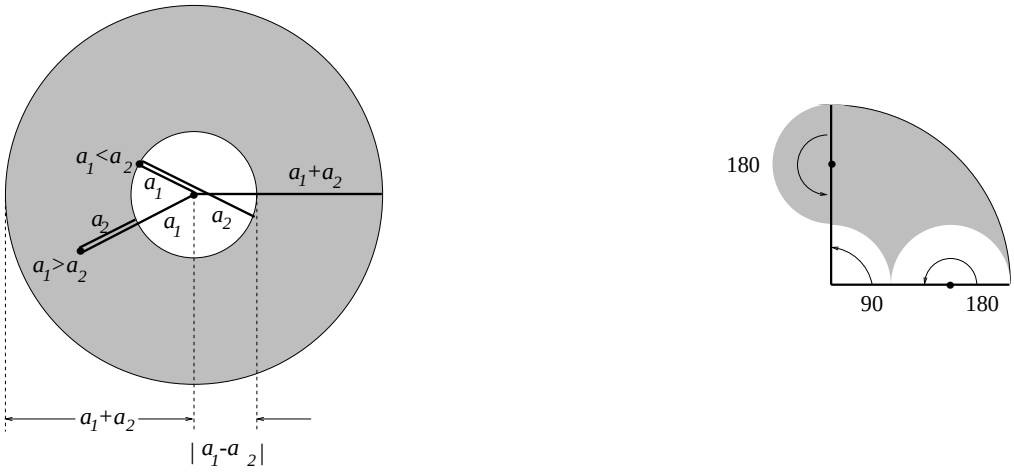

(A) (B)

Figure 5.9: Workspace of two-link planar manipulator: (A) no joint limits. (B) Joint limits of $0 \leq \theta_1 \leq \pi/2$ and $0 \leq \theta_2 \leq \pi$.

where the elements of ${}^3\mathbf{R}_6 = \{r_{ij}\}$ are now known. Simply apply the solution for the spherical manipulator of Section 5.3 to find $\theta_4, \theta_5, \theta_6$.

In total, there are $8 = 2 \times 2 \times 2$ solutions for the inverse kinematics for the 6R arm: 2 for the shoulder (leftie/rightie), 2 for the elbow (up and down), and 2 for the wrist.

5.5 Workspace

Workspace is the set of configurations that a manipulator can assume. Workspace depends on the joint limits and on the presence of obstacles. For the planar 2-link manipulator without joint limits, the workspace is a hollow disk, regardless of the relative length of a_1 versus a_2 (Figure 5.9(A)). The outer boundary of the disk has radius $a_1 + a_2$, while the inner boundary has radius $|a_1 - a_2|$. For a given absolute difference $|a_1 - a_2|$, the inner boundary radius holds whether $a_1 < a_2$ or $a_1 > a_2$.

With joint limits (e.g., $0 < \theta_1 < 90^o$ and $0 < \theta_2 < 180^o$), only a portion of this hollow disk can be reached (Figure 5.9(B)).

Consider now a spatial 2-link manipulator, where $\mathbf{z}_1 \perp \mathbf{z}_0$ and $a_1 > a_2$ (Figure 5.10). Rotation of the endpoint about $\mathbf{z}_1$ generates a circle of radius a_2. Rotation about axis $\mathbf{z}_0$ sweeps the circle to form a torus (Figure 5.10(B)); only half of the torus is shown in the figure. The workspace of the endpoint lies on the surface of the torus.

5.5.1 Holes and Voids

Consider a 3-link spatial manipulator formed by adding a link to the 2-link spatial manipulator above, so that $\mathbf{z}_2 \parallel \mathbf{z}_3$ and $a_3 \neq 0$ (Figure 5.11). Suppose $a_1 > a_2 + a_3$ and $a_2 > a_3$. Joints 2 and 3 are like the planar 2-link manipulator, and sweep out a hollow disk. Joint 1 sweeps the hollow disk to form a torus (Figure 5.11(B)).

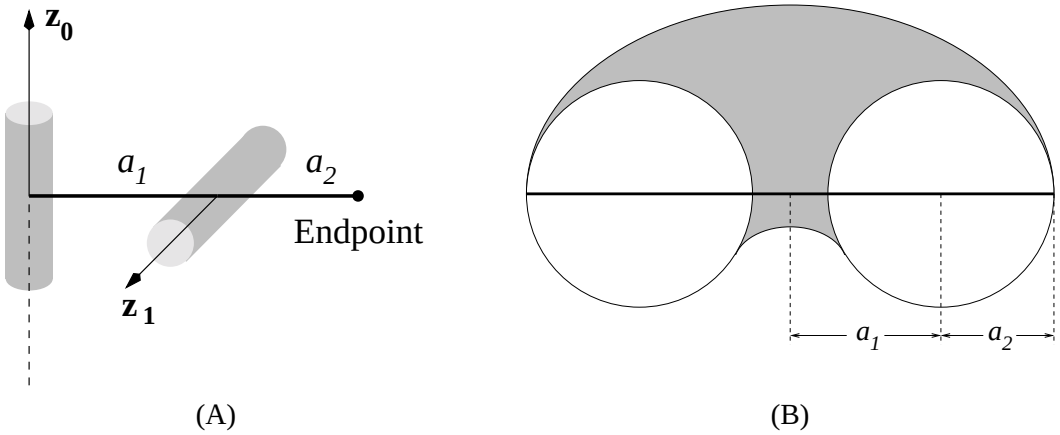

Figure 5.10: A spatial 2R manipulator (A) and its workspace (B).

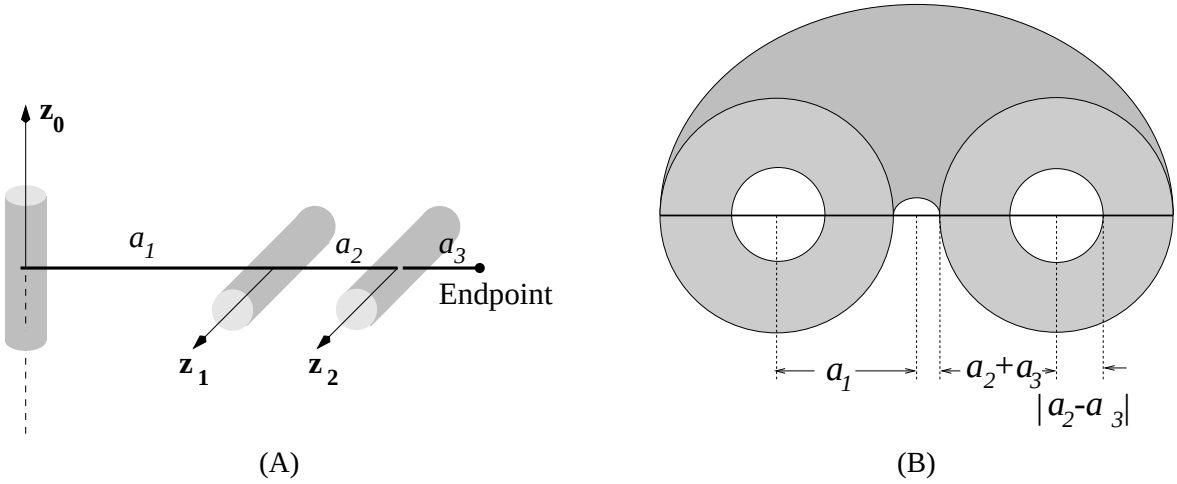

Figure 5.11: A spatial 3R manipulator (A) and its workspace (B).

The donut hole is called a *hole*. The empty space in the interior of the donut is called a *void*. Voids are considered much worse than holes, because they are interior to the workspace and pose a difficult for trajectory planning. Manipulator designers attempt to avoid voids by setting $a_2 = a_3$. The hole on the other hand represents the workspace boundary, and there has to be a workspace boundary someplace.

The donut hole can be minimized by setting $a_1 = a_2 + a_3$. Alternatively, if $a_1 = 0$ and $a_2 = a_3$, then the workspace is a perfect sphere. The manipulator in Figure 5.11(A) is the same as the first 3 joints of the elbow robot. Commercial elbow robots are typically designed with these criteria to avoid holes and voids.

5.5.2 Total, Primary, and Secondary Workspace

So far, we have only considered position. Consider now the elbow manipulator, where we also have to consider orientation of the end link as well as position of the endpoint. In Figure 5.12, we have depicted the last three joints as a ball joint to suggest the spherical joint equivalent (Figure 5.12(A)). The length of the end link from wrist to endpoint is d_6.

The *total* or *reachable workspace* is the positioning workspace, without regard for orientation. Suppose

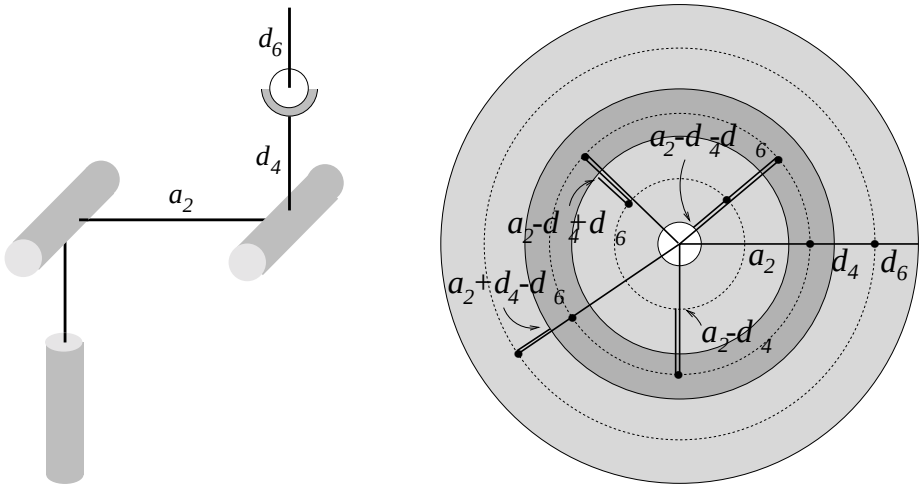

(A) (B)

Figure 5.12: Elbow robot with last three joints depicted as a ball joint.

$a_2 > d_4 > d_6$ and $a_2 > d_4 + d_6$. Then the reachable workspace is a hollow sphere with outer radius $a_2 + d_4 + d_6$ and inner radius $a_2 - d_4 - d_6$, Figure 5.12(B) shows a cross-section of the workspace sphere through its center; the total of all shaded areas represents the reachable workspace. The endpoint can achieve all positions in these shaded areas.

The *primary workspace* comprises points reachable in all orientations. For the elbow manipulator, the primary workspace has an outer radius $a_2 + d_4 - d_6$ and an inner radius $a_2 - d_4 + d_6$; in Figure 5.12(B) the dark-shaded area represents the primary workspace. When the wrist point is located in the primary workspace, any orientation of the end link may be achieved. Notice how small the primary workspace is.

The *secondary workspace* is the total workspace minus the primary workspace. The secondary workspace comprises points that can be reached in only partial orientations. For the elbow manipulator, the secondary workspace is a hollow sphere with outer radius $a_2 + d_4 + d_6$ and inner radius $a_2 + d_4 - d_6$ plus another hollow sphere with outer radius $a_2 - d_4 + d_6$ and inner radius $a_2 - d_4 - d_6$. The light-shaded areas in Figure 5.12(B) depict the secondary workspace.